A General Fluid Dynamic Analysis of Drop Ejection in Drop-on-Demand Ink Jet Devices

James Q. Feng

Xerox Corporation, Wilson Center for Research and Technology, Webster, New York

Drop-on-demand devices are the heart of most modern ink jet printers. The fluid dynamic process during drop ejection is complex with time-dependent fluid interface disruptions. Based on computations with a generic problem configuration, the present work attempts to provide an insight into the drop ejection behavior for establishing general design rules in device development. The computational results show that the volume of ejected drop is very close to the volume of fluid pushed through the nozzle by an actuation pulse. The speed of the ejected drop is typically between one third and two thirds of the average velocity of the fluid pushed through the nozzle during actuation. The conditions for obtaining various (desirable or undesirable) drop shapes immediately after ejection are examined. The cases when drops may not be successfully ejected are also discussed.

Introduction

The rapid growth of ink jet printing market has motivated tremendous efforts in searching for new means of further improving image quality and reducing device cost.[1] Understanding the fluid dynamic process of drop formation and drop ejection becomes more than ever important to successful research and development of new ink jet printheads. There are two main types of ink jet devices, namely, the continuous–jet type and drop-on-demand type.[1,2] In a continuous-jet device, the liquid emerging from the nozzle continually in the form of a jet that subsequently disintegrates into a train of drops. Sophisticated electrical signals are needed to control both the amount of electric charge on each individual drop and direction of motion of each drop from the continuous jet. In contrast, a drop-on-demand device uses electrical signals just to control the actuation at the moment when an individual drop is ejected. Because of its great fundamental simplicity, the drop-on-demand type has gained popularity in most modern ink jet printers. Hence, the present work focuses on the basic drop ejection process in drop-on-demand devices.

Typically, a drop-on-demand device consists of a fluid chamber with an opening called a nozzle from where drops are to be generated under actuation. The basic function of actuation is to push a certain amount of the liquid out of the fluid chamber through the nozzle. If the liquid pushed out of the nozzle gains enough forward momentum to overcome the surface tension restoring effect, a drop can be ejected. In the ideal drop ejection cycle, the fluid in the chamber is initially at rest, driven into motion to eject a drop in response to an electrical command, and back to the original rest state after refilling from ink reservoir and viscous damping.[3]

The basic mechanism of actuation is to convert the electrical signal (typically in the form of a pulse) into mechanical motions of fluid. For example, in a piezoelectric ink jet device, the fluid motion is driven by the electrically controlled solid wall movements.[3,4] In a thermal ink jet device, the fluid motion is driven by the bubble expansion induced through an electrically controlled micro-heating element.[5,6] More recently, a micro-electro-mechanical diaphragm has been considered as a possible energy efficient actuation method.[7,8] Although the overall device configuration can vary significantly to accommodate the specific actuation method, the fluid dynamics of drop ejection, especially near the nozzle region, is essentially the same for most of the drop-on-demand devices. Therefore, the present analysis of the fluid dynamic behavior of drop ejection is focused on a somewhat idealized, generic fluid chamber configuration with the nozzle on one end and an open fluid inlet on the other that allows liquid to be pushed in and out, representing situations with almost any actuation methods.

Theoretically, the drop ejection phenomenon is governed by Navier–Stokes equations with appropriate boundary conditions describing fluid interface motions.[9] Due to the nonlinearities arising from inertia, capillarity, and coupling of the free surface kinematics to the flow field, conventional methods cannot be used to obtain the desired mathematical solutions. Therefore, the complex fluid dynamic process during drop ejection is simulated with a CFD (Computational Fluid Dynamics) package FLOW-3D[10] that employs the VOF (Volume-
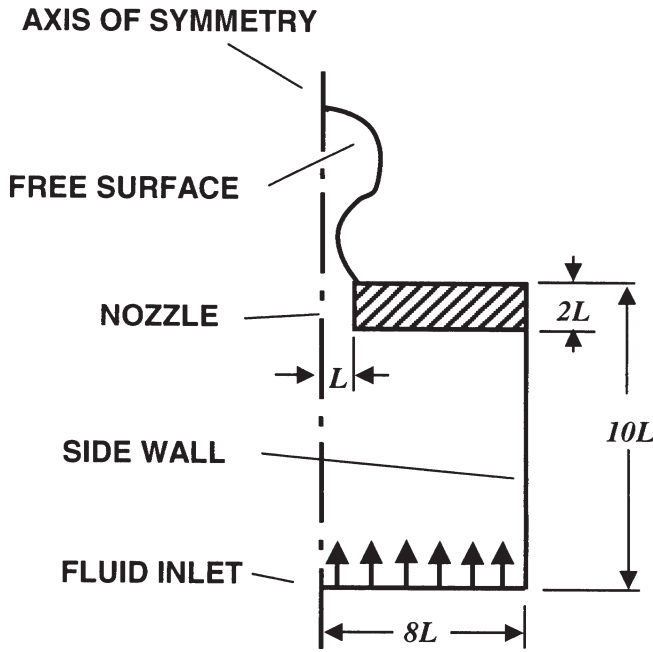
Figure 1. Schematic of the problem configuration: an axisymmetric drop ejection chamber.

of-Fluid) method[11] to track effectively the transient fluid interface deformations and disruptions. To provide physical insights for establishing general design rules in device development, the primary attention here is paid to variables of immediate practical importance such as the volume and speed, as well as shape evolution of ejected drops.

Theoretical Description

It is well accepted that the fluid dynamic behavior of drop ejection is governed by the Navier–Stokes equations with appropriately specified boundary conditions. It is also reasonable to assume the fluid is incompressible. Because the speed of acoustic waves in liquids, e.g., water, is about 1500 m/s, the wavelength for a frequency of even 1 MHz is still about 1.5 mm, much greater than the length scale of the sizes of the nozzle and drop in most ink jet devices. Restricting the theory to Newtonian fluids can of course help reduce the complexity of the problem. Written in terms of nondimensional variables, the Navier–Stokes equations take the form

$$\mathrm{Re}\left(\frac{\partial \underline{v}}{\partial t} + \underline{v} \cdot \nabla \underline{v}\right) = \nabla \cdot \left[-p\underline{\underline{I}} + \nabla \underline{v} + (\nabla \underline{v})^T\right] \quad (1)$$

with the incompressibility constraint

$$\nabla \cdot \underline{v} = 0 \quad (2)$$

where t is time in units of a characteristic time T, $\underline{v}$ is the fluid velocity vector in units of a characteristic velocity U (defined after Eq. 7), p is pressure in units of $\mu U/L$ with μ denoting the viscosity of ink and L the characteristic length scale of the system, $\underline{\underline{I}}$ is the identity tensor, and $\mathrm{Re} = \rho U L/\mu$ is the Reynolds number with ρ denoting the density of ink.
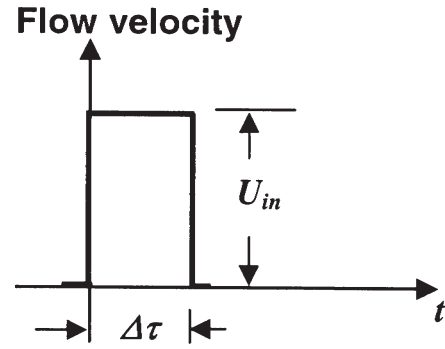

Figure 2. The assumed inlet flow velocity as a function of time.

To preserve the generality of the analysis, a drop ejection system of axisymmetric configuration shown in Fig. 1 is considered. Here, we basically have a fluid chamber with a drop formation nozzle and an open fluid inlet that allows the ink to be pushed in and out of the chamber to simulate an actuation mechanism for drop ejection. For simplicity, the incoming flow at the fluid inlet is specified with a plug flow profile. Besides the usual boundary conditions such as no-slip and no-penetration at solid walls for fluid confinement, we need to specify the traction boundary condition at the fluid free surface to guarantee the conservation of momentum

$$\underline{n} \cdot \left[-p\underline{\underline{I}} + \nabla \underline{v} + (\nabla \underline{v})^T\right] = \frac{1}{Ca}\,\underline{n}\nabla \cdot \underline{n} \quad (3)$$

where $\underline{n}$ is the local unit normal vector at the fluid free surface and Ca = $\mu U/\gamma$ is the capillary number with γ denoting the surface tension.

Because the fluid is incompressible, the amount of the fluid coming into the chamber from the inlet boundary must go out of the nozzle. Whether the fluid going out of the nozzle can form a drop, and if formed, the properties of the drop such as volume, velocity, and initial shape, must depend on the parameters that describe the actuation conditions represented by the fluid flow at the inlet boundary. Again, the problem under consideration is kept as simple as possible by assuming the incoming fluid at the inlet boundary takes the velocity form of a square pulse (as indicated in Fig. 2). Thus, two parameters are sufficient to describe the incoming fluid flow at the fluid inlet boundary: one is the incoming flow rate Q; the other is the duration of the square pulse $\Delta\tau$. For the configuration in Fig. 1, the uniform velocity of the plug–flow profile at the inlet boundary is then given by

$$U_{in} = Q/(64\,\pi) \quad (4)$$

and the amount (volume) of the incoming fluid during actuation is given by

$$V = Q\,\Delta\tau = 64\,\pi\,U_{in}\,\Delta\tau , \quad (5)$$

where the parameters are all made dimensionless with U_{in} measured in units of U, $\Delta\tau$ in units of T, V in units of L^3, and Q in units of L^3/T. Another important quantity is the average velocity of the fluid pushed through the nozzle during actuation, defined here for the configuration in Fig. 1 as
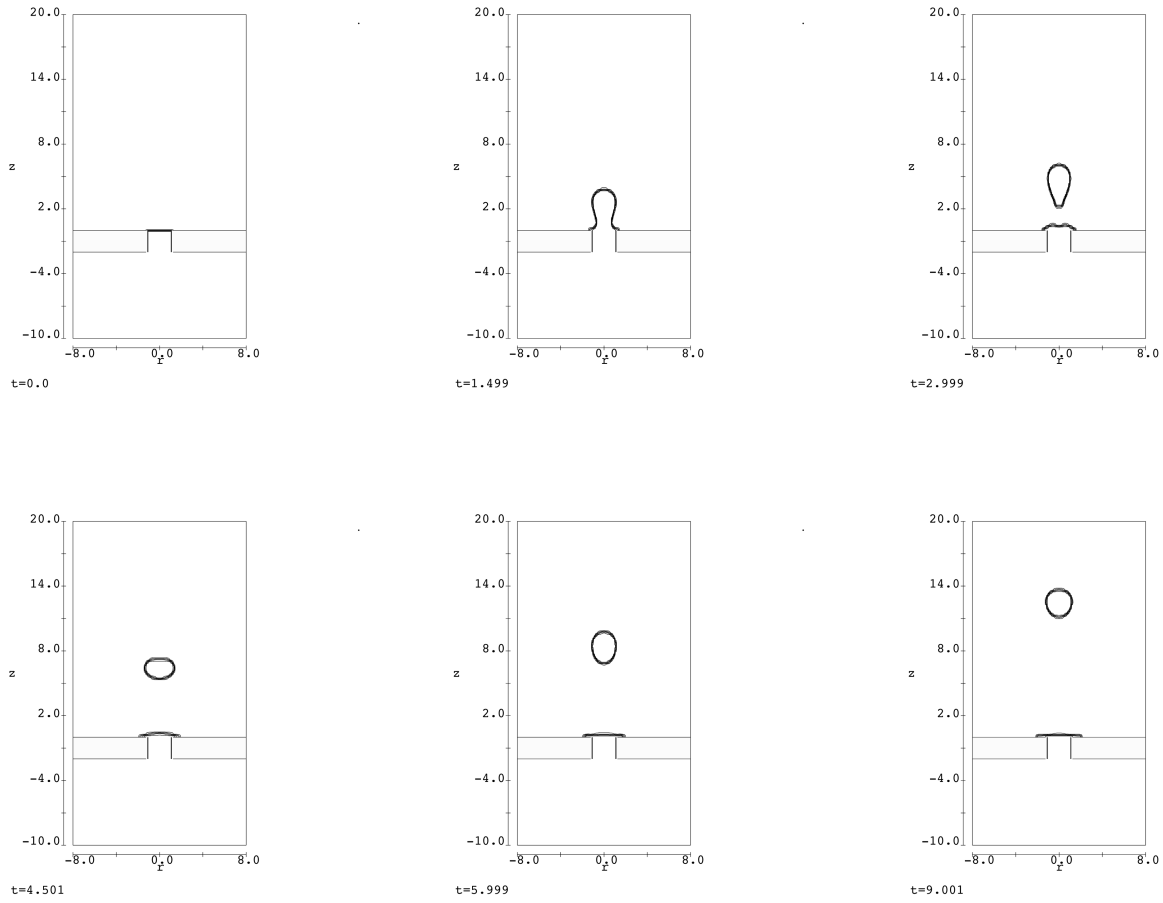
$$U_n = Q/\pi \quad (6)$$

Figure 3. Time sequence of drop ejection with $Q = 10$ and $\Delta\tau = 1.0$, i.e., $V = 10$, $U_n = 3.2$, for Re $= 12.5$ at $t = 0$, 1.5, 3.0, 4.5, 6.0, and 9.0.

in units of U.

As might be noted, the present velocity form of the incoming fluid assumed at the inlet boundary (cf. Fig. 2) represents only half of a typical actuation cycle, which usually consists of both a "forward" stroke and a "backward" stroke. The "forward" stroke is by design to push the fluid out of the nozzle to eject a drop, whereas the "backward" stroke is a consequence of the actuator returning to the original position to be ready for the next actuation. With the surface tension effect, the "backward" stroke also helps refill ink into the fluid chamber. Based on their functions, the "forward" stroke drives the drop ejection process whereas the "backward" stroke induces the ink refilling process. If the ink refilling process, which can become quite complicated in its own right, is left open for future analysis, we can then keep the present attention focused on the generic behavior of drop ejection under an idealized actuation with a simple "forward" stroke.

To further reduce the complexity of the analysis, it is often desired to find ways to eliminate some of the independent parameters. For the present problem, it is advantageous to use the timescale for capillary driven fluid motions $(\rho L^3/\gamma)^{1/2}$, as the characteristic time T. Then, we can naturally reduce the two apparently independent parameters Re and Ca in Eqs. 1 and 3 into one, such as

$$1/\text{Ca} = \text{Re} = (\rho L\, \gamma)^{1/2}/\mu, \qquad (7)$$

with U being defined as L/T. Thus, the drop ejection be-

havior is totally controlled by three independent parameters: Re, Q, and $\Delta\tau$ for the problem configuration and given form of inlet flow under consideration. The value of Re reflects the ink material properties and the geometric size of the nozzle, whereas Q and $\Delta\tau$ describe the actuation conditions.

Numerical Results and Discussion

As a convenient reference, the characteristic length may be considered as $L = 10^{-5}$ m, i.e., a 20 μm diameter nozzle). Thus, the corresponding characteristic volume would be 10^{-15} m³, i.e., 1 pL. If the surface tension, density, and viscosity of the ink are respectively assumed as $\gamma = 6.25 \times 10^{-2}$ N/m, $\rho = 10^3$ kg/m³, and $\mu = 2 \times 10^{-3}$ Ns/m², i.e., that of a typical aqueous ink, we should have Re $= 12.5$ and $T = 4 \times 10^{-6}$ s. In all FLOW-3D computations presented here, the contact angle is assumed to be 15° on the solid nozzle plate. The ADI line implicit pressure iteration scheme in both (x– and z–) directions and the implicit scheme for viscous stress calculation[10] are used. Taking $Q = 10$ ($U_{in} = 0.05$) and $\Delta\tau = 1.0$ (corresponding to a dimensional flow rate at inlet boundary of about 2.5×10^{-9} m³/s and a time duration of 4 μs in actuation, respectively) yields $V = 10$, i.e., a 10 pL volume of fluid being pushed through the nozzle, according to Eq. 5. The FLOW-3D computational results for such a case are shown in Fig. 3. By comparing the results between $t = 0$ and 3.0, it is found that after the drop is ejected the fluid level at the nozzle is a little
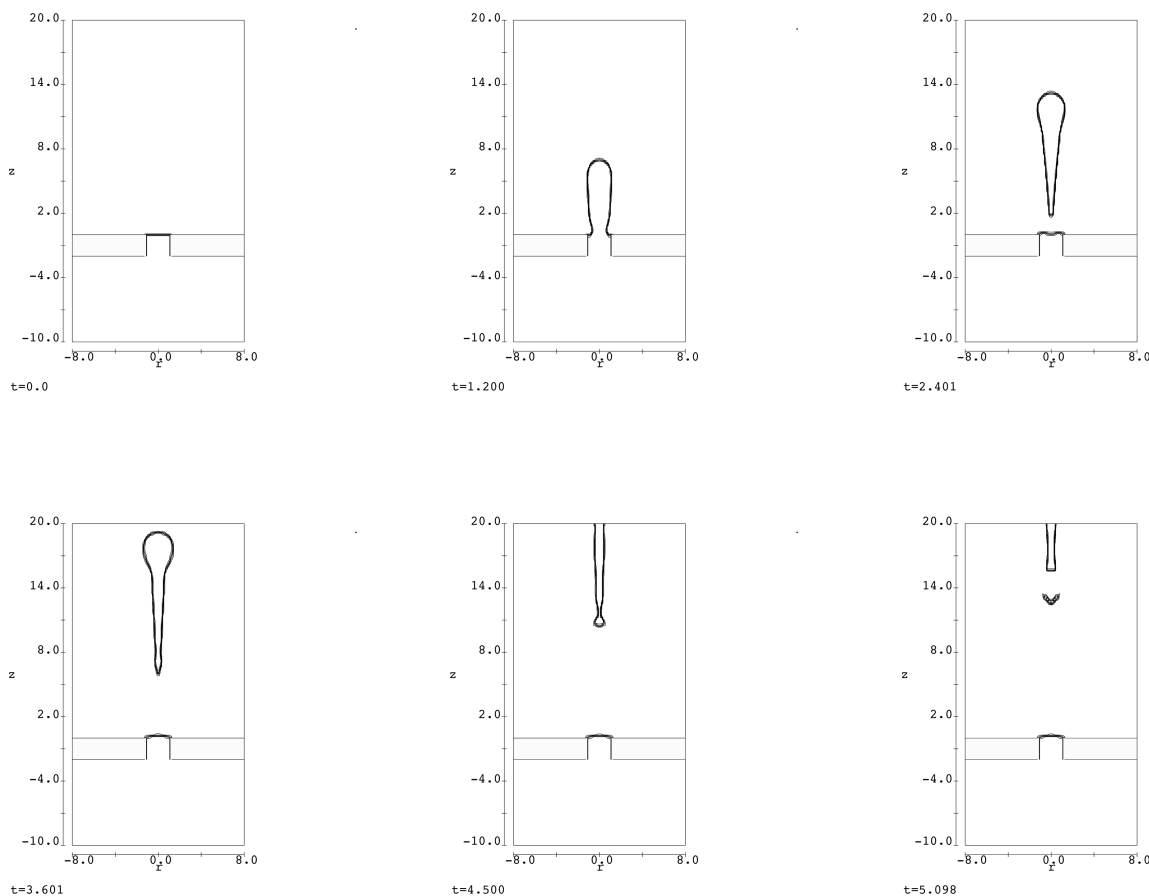
Figure 4. Time sequence of drop ejection with $Q = 20$ and $\Delta\tau = 1.0$, i.e., $V = 20$, $U_n = 6.4$, for Re = 12.5 at $t = 0, 1.2, 2.4, 3.6, 4.5,$ and 5.1.

higher than that in the original state, indicating that the volume of the ejected drop is about 9–10% less than the amount of fluid pushed through the nozzle. By examining the results at $t = 6.0$ and 9.0, we obtain the drop speed of about 1.4, less than $U_n/2$, and corresponding to a dimensional speed of about 3.5 m/s. The timescale for the drop to detach from the nozzle is about 2.8 for this case, despite the fact that actuation pulse terminates much earlier at $t = 1.0$.

The situation for $Q = 20$ (with other parameters kept the same as in Fig. 3) is shown in Fig. 4 where the volume of fluid pushed through the nozzle is $V = 20$. A drop of volume about 19.5 is ejected with a speed of about 5.0 (about 0.8 U_n). The complete drop detachment from the nozzle meniscus occurs at $t = 2.2$. Because of the higher velocity of the fluid through the nozzle, the ejected drop moves at higher speed and develops a long tail that integrates into small droplets at about $t = 5.1$. In view of the cases shown in Figs. 3 and 4, it appears that the volume of the ejected drop is very close to the value of V, the volume of fluid pushed through the nozzle. If in fact the drop size is controlled by $V = Q\,\Delta\tau$, a drop of about the same volume as that in Fig. 4 could be expected by the choices of $Q = 10$ and $\Delta\tau = 2.0$ instead of $Q = 20$ and $\Delta\tau = 1.0$ as in Fig. 4. This is indeed the case as seen in Fig. 5. However, the drop moves slower and the tail, although not as long, breaks into a small droplet at about $t = 5.2$. Interestingly, this small droplet moves slightly faster than the main drop such that at about $t = 8.0$ it catches

up and coalesces into the main drop. But the tail of the drop develops into a skirt shape that is unstable and at about $t = 9.5$ it breaks again into smaller droplets as seen in Fig. 5. In this case, the drop completes the detachment from the nozzle meniscus at about $t = 4.3$. The speed of the ejected drop in Fig. 5 is about 2.0 (about 0.6 U_n), much lower than that in Fig. 4.

From the physical point of view, the speed of the ejected drop must correlate with U_n as defined in Eq. (6), which defines the average velocity of the fluid pushed through the nozzle that eventually forms the drop. For $Q = 10$ and 20, $U_n = 3.2$ and 6.4, respectively, the cases shown in Figs. 3–5 indicate that the speed of an ejected drop is a fraction of the value of U_n; a loss of momentum must therefore have occurred during the drop formation process. As seen from Figs. 3–5, the momentum input from the actuation finishes on a much shorter timescale than the time for the drop to completely detach from the nozzle. There is a considerable adjustment of the amount of momentum in the ejected drop during its formation process, especially after the actuation ceases and before the complete detachment of the drop from the nozzle. Such a momentum adjustment mainly arises from the capillary force that tends to hinder the continuing forward protrusion of the meniscus. The capillary effect combined with the viscous effect in the fluid give rise to a momentum redistribution in the fluid outside the nozzle, which yields less forward momentum of the ejected drop than the net momentum
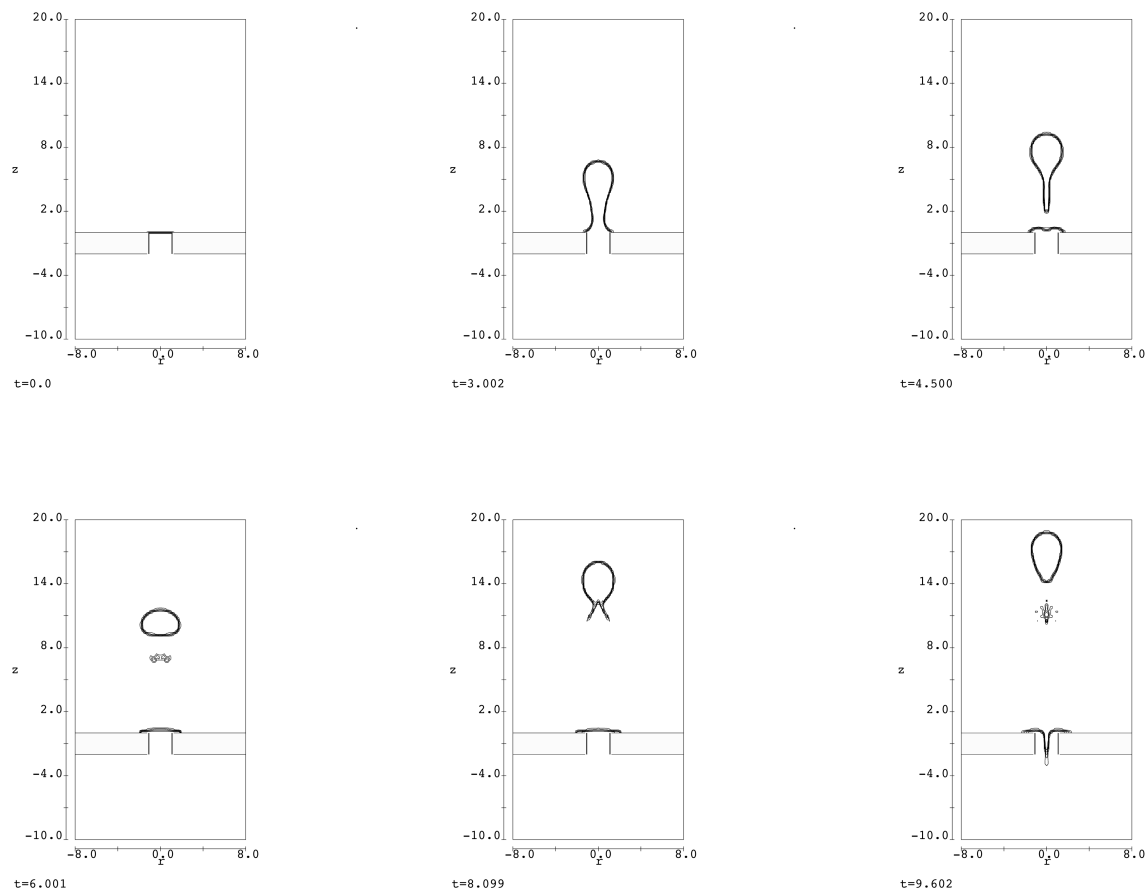
Figure 5. Time sequence of drop ejection with $Q = 10$ and $\Delta\tau = 2.0$, i.e., $V = 20$, $U_n = 3.2$, for Re = 12.5 at $t = 0$, 3.0, 4.5, 6.0, 8.1, and 9.6.

input from the actuation. Accordingly, the drop speed increases with the size of ejected drop for a given value of U_n because of weakened capillary effect via smaller meniscus curvatures.

Shown in Fig. 6 is a smaller drop (of volume about 4.5) ejected with $Q = 10$ and $\Delta\tau = 0.5$ with other parameters kept the same as that in Fig. 3. For the same value of U_n (= 3.2), the drop in Fig. 6 (with a small size) barely moves after ejection. It oscillates with large amplitudes and breaks up after $t = 8.0$. The case shown in Fig. 6 represents a practically unsuccessful drop ejection for ink jet applications, even though a drop is somehow generated by the actuation. Drops of the same size as that in Fig. 6 can also be generated with $Q = 20$ and $\Delta\tau = 0.25$, as shown in Fig. 7. Because of the higher value of U_n in this case, the drop of volume of about 4.8 moves at a speed of about 3.2 (about 0.5 U_n) after ejection. But the drop, completing detachment from nozzle meniscus at $t = 1.5$, breaks into two pieces after $t = 4.0$. If we set $Q = 20$ and $\Delta\tau = 0.125$, a smaller drop (with volume of about 2.3) is generated. But, similar to that seen in Fig. 6, this drop barely moves, and the drop ejection should be regarded as practically unsuccessful. It seems that a higher flow rate is required for successful ejection of smaller drops.

Although drops of larger size appear to be easier to generate, it does not seem to be as easy to obtain either large or small drops at Re = 12.5 without some level of

disintegration (except as seen in Fig. 3). For small drops, the large momentum density, i.e., local fluid velocity, required for drop ejection transforms into forces that can cause large amplitude drop oscillations with drop disintegration ensuing (cf. Fig. 7). For large drops, the surface tension effect is relatively weak so it becomes difficult to retain the fluid in an integrated drop even without large momentum density. Figure 8 shows a fairly large drop ejected with $Q = 10$ and $\Delta\tau = 4.0$. The drop of volume about 39, detached from the nozzle meniscus at about $t = 6.0$ and moving at a speed of about 2.0 (about 0.6 U_n), disintegrates into two sizable fragments after $t = 9.0$. If $Q = 20$ and $\Delta\tau = 2.0$ are used, however, an ejected drop of volume about 40 would disintegrate only at the tip of its tail, leaving small satellite droplets one after another behind it similar to that seen in Fig. 4.

If the Reynolds number is reduced to unity (Re = 1), drop ejection with $Q = 10$ and $\Delta\tau = 1.0$ (the same actuation conditions as that for Fig. 3) becomes impossible, even though a volume of fluid, $V = 10$, is pushed through the nozzle during actuation. Under these conditions the disruption of fluid interface cannot happen because fluid momentum is insufficient to overcome the relatively more significant viscous effect. An increase in flow rate Q is needed for successful drop ejection at Re = 1. For example, a drop of volume about 10 can be generated with $Q = 20$ and $\Delta\tau = 0.5$ at Re = 1 as shown in Fig. 9.

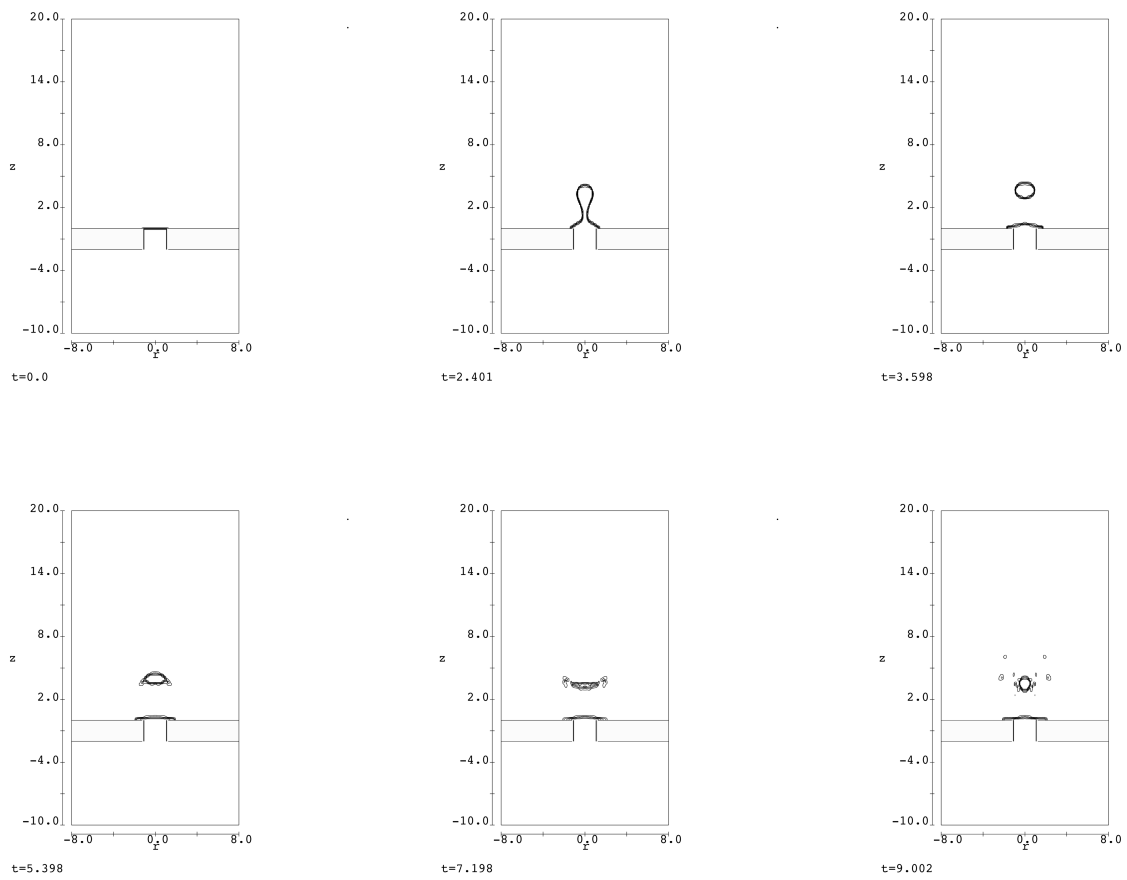**Figure 6.** Time sequence of drop ejection with $Q = 10$ and $\Delta\tau = 0.5$, i.e., $V = 5$, $U_n = 3.2$, for Re = 12.5 at $t = 0$, 2.4, 3.6, 5.4, 7.2, and 9.0.
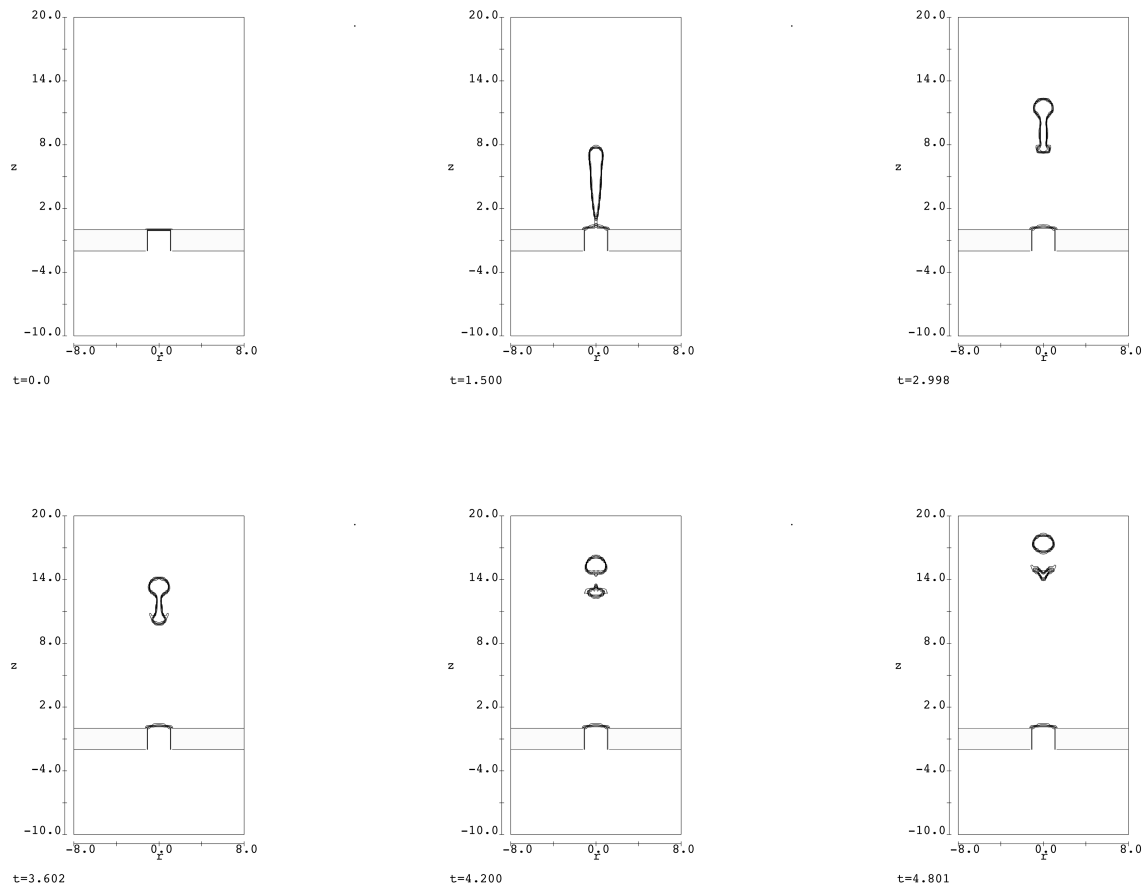

Figure 7. Time sequence of drop ejection with $Q = 20$ and $\Delta\tau = 0.25$, i.e., $V = 5$, $U_n = 6.4$, for Re = 12.5 at $t = 0$, 1.5, 3.0, 3.6, 4.2, and 4.8.
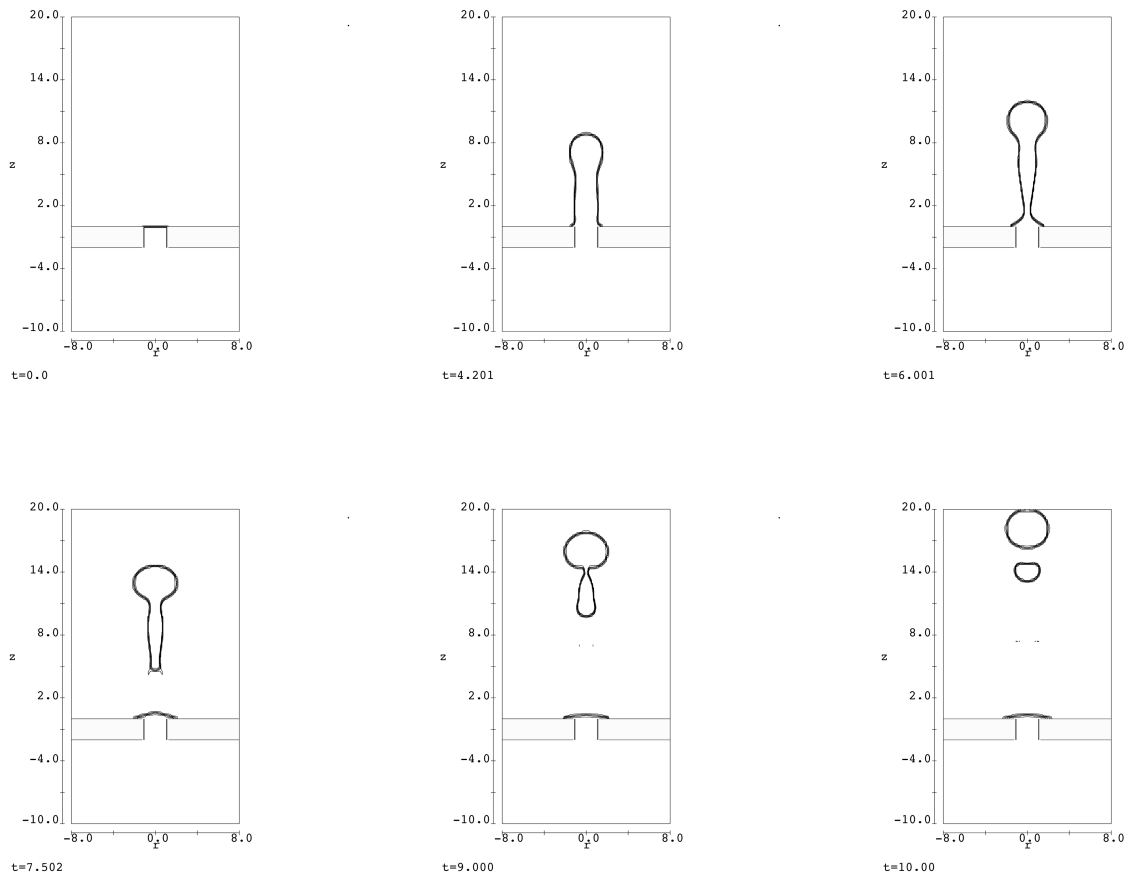
Figure 8. Time sequence of drop ejection with $Q = 10$ and $\Delta\tau = 4.0$, i.e., $V = 40$, $U_n = 3.2$, for Re = 12.5 at $t = 0, 4.2, 6.0, 7.5, 9.0$, and 10.0.
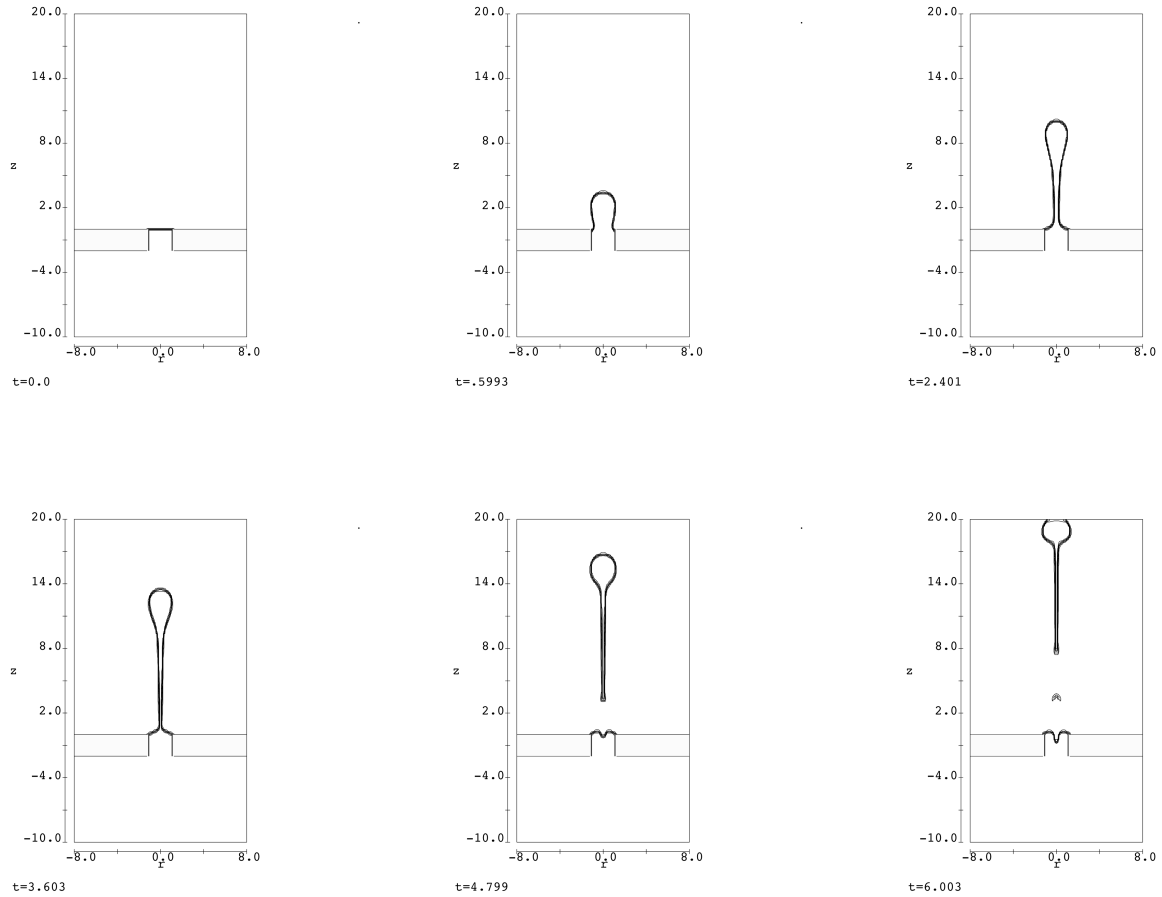

Figure 9. Time sequence of drop ejection with $Q = 20$ and $\Delta\tau = 0.5$, i.e., $V = 10$, $U_n = 6.4$, for Re = 1 at $t = 0, 0.6, 2.4, 3.6, 4.8$, and 6.0.
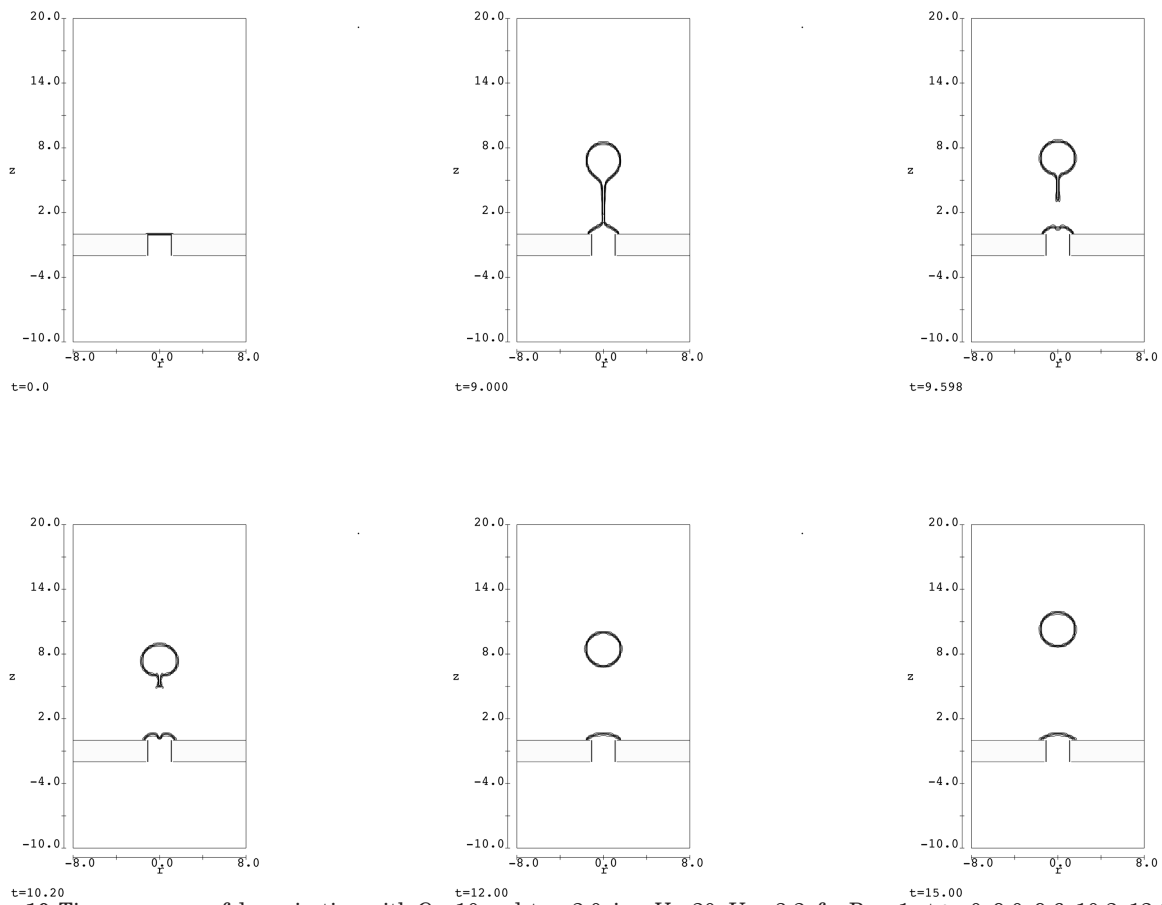
Figure 10. Time sequence of drop ejection with $Q = 10$ and $\Delta\tau = 2.0$, i.e., $V = 20$, $U_n = 3.2$, for Re = 1 at $t = 0, 9.0, 9.6, 10.2, 12.0$, and 15.0.
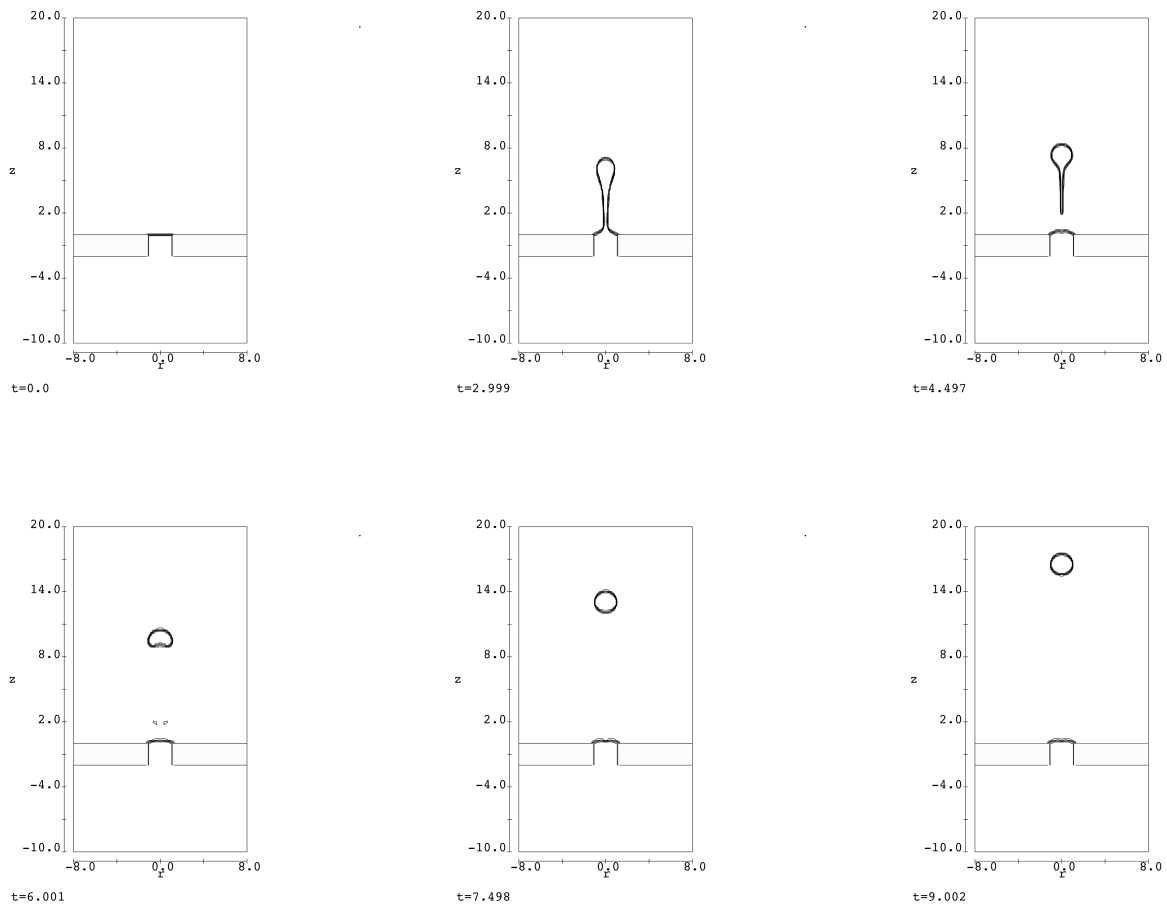

Figure 11. Time sequence of drop ejection with $Q = 20$ and $\Delta\tau = 0.25$, i.e., $V = 5$, $U_n = 6.4$, for Re = 1 at $t = 0, 3.0, 4.5, 6.0, 7.5$, and 9.0.
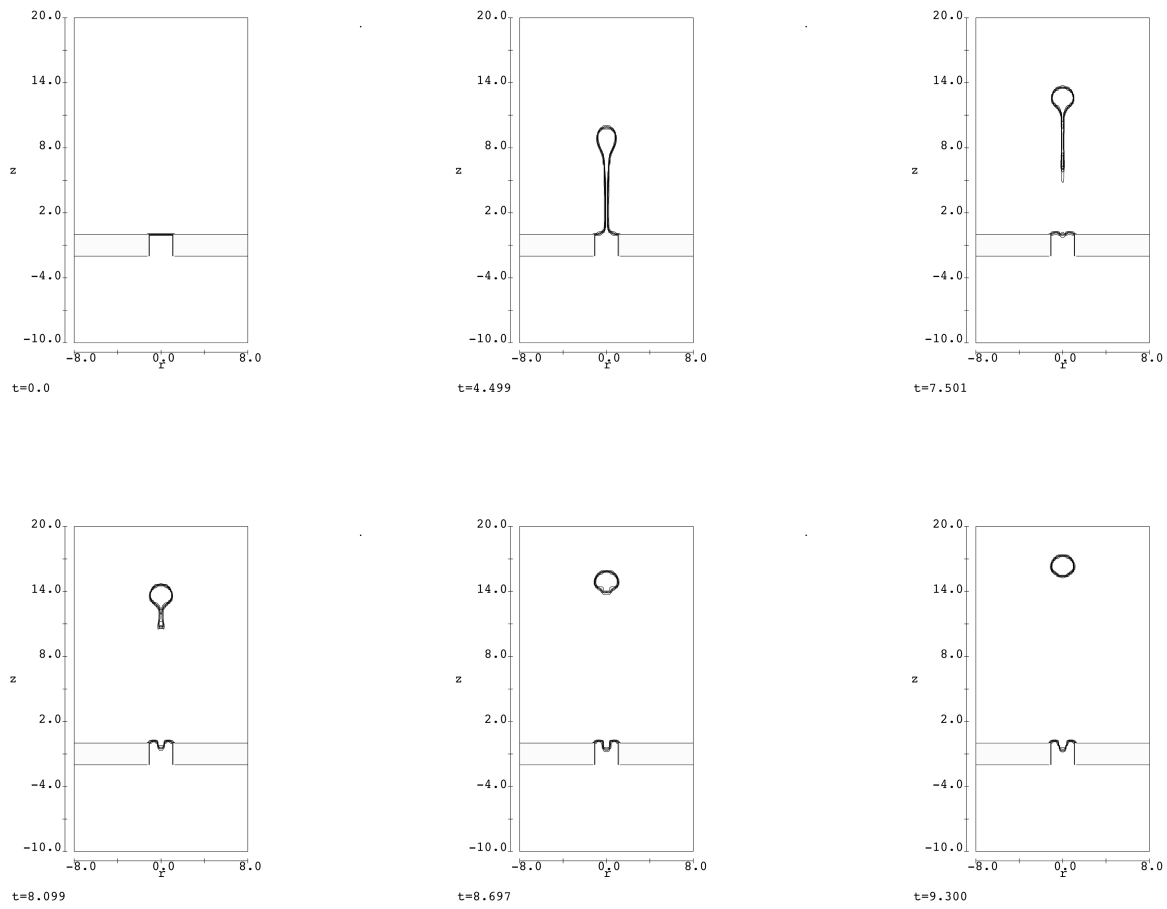
Figure 12. Time sequence of drop ejection with $Q = 30$ and $\Delta\tau = 1/6$, i.e., $V = 5$, $U_n = 9.6$, for Re = 0.5 at $t = 0$, 4.5, 7.5, 8.1, 8.7, and 9.3.
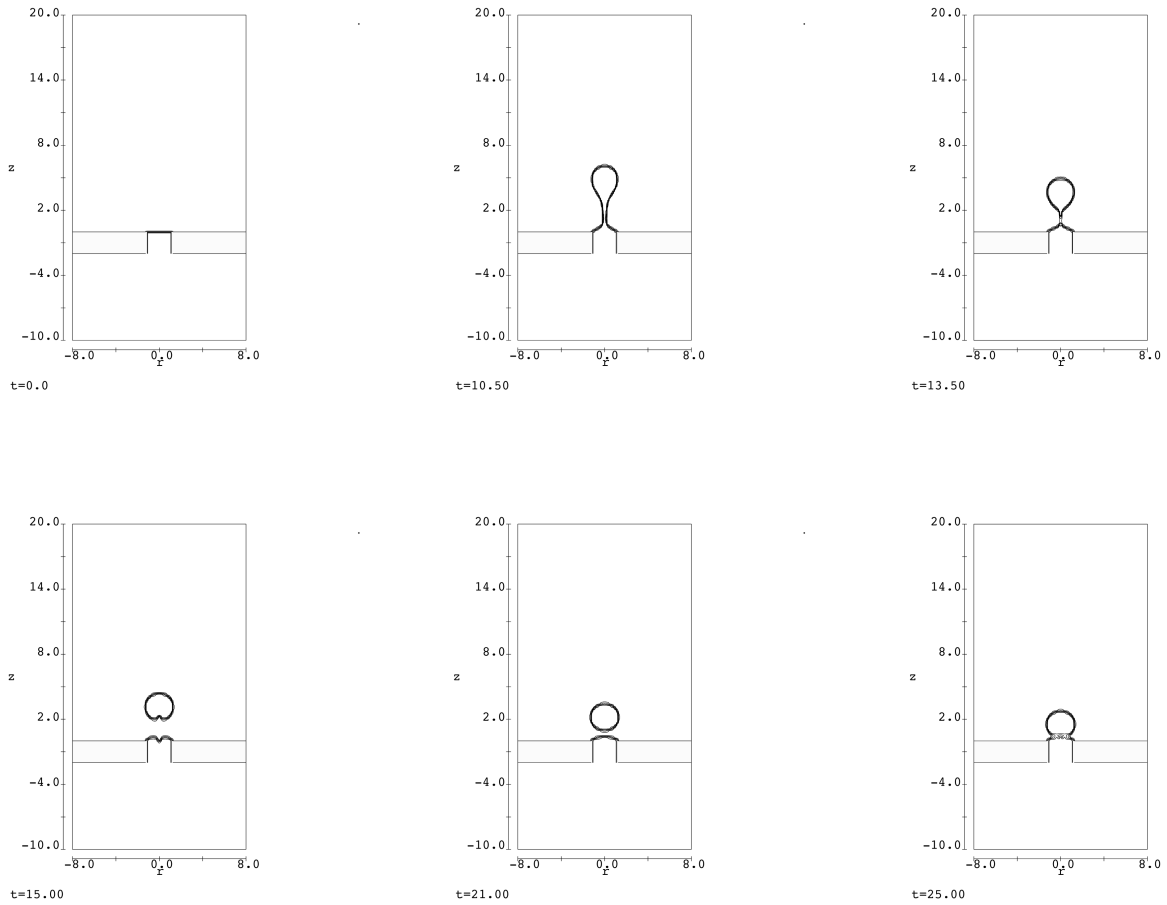

Figure 13. Time sequence of drop ejection with $Q = 20$ and $\Delta\tau = 0.5$, i.e., $V = 10$, $U_n = 6.4$, for Re = 0.35 at $t = 0$, 10.5, 13.5, 15.0, 21.0, and 25.0.
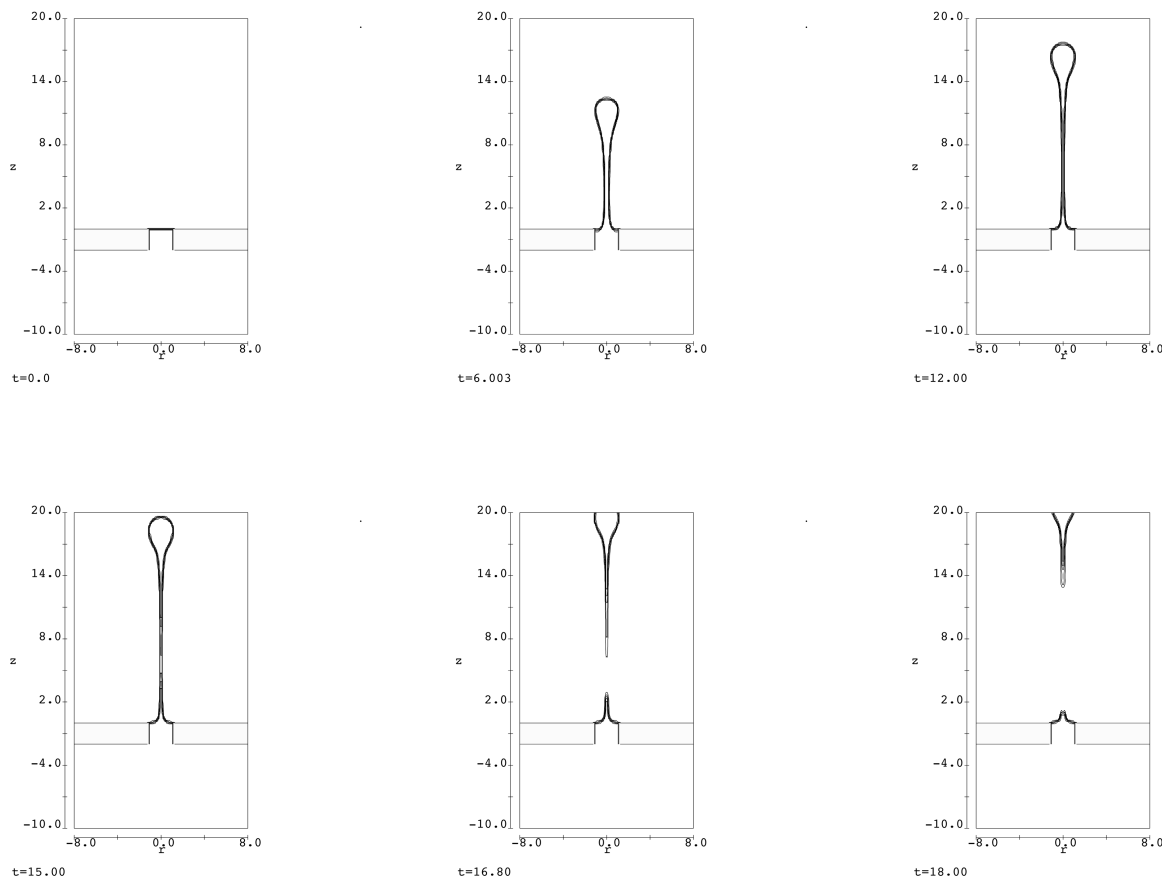
Figure 14. Time sequence of drop ejection with $Q = 40$ and $\Delta\tau = 0.25$, i.e., $V = 10$, $U_n = 12.8$, for Re = 0.125 at $t = 0$, 6.0, 12.0, 15.0, 16.8, and 18.0.

The drop moves at a speed of about 2.9 (about 0.5 U_n), after detaching from the nozzle at about $t = 4.6$ with a thin, long tail that disintegrates into small satellite droplets as it proceeds. With $Q = 10$ and $\Delta\tau = 2.0$, however, a drop of volume about 19 can be ejected at Re = 1 with a slow speed of about 0.6 (about 0.2 U_n), as shown in Fig. 10. In this case, the actuation is so gentle that the drop can retain a nice round shape all the time. But gentle actuation cannot be used for the effective ejection of small drops. Even with $Q = 20$, a drop of volume less than 3.5 cannot be successfully generated at Re = 1. Figure 11 shows a drop of volume about 4.5 generated with $Q = 20$ and $\Delta\tau = 0.25$, moving at a speed about 2.7 (less than 0.5 U_n) after ejection. Comparing with the drop in Fig. 7 at Re = 12.5, under the same actuation condition, the drop in Fig. 11 (at Re = 1) moves at a slower speed, but it retains a nice round shape without serious disintegration.

If the value of Re is reduced further to 0.5, no fluid interface disruption would occur (and therefore no drop would be generated) with the actuation condition of $Q = 20$ and $\Delta\tau = 0.25$. The flow rate Q needs to be increased to eject a drop of $V = 5$. Figure 12 shows the case with $Q = 30$ and $\Delta\tau = 0.167$ at Re = 0.5 where a drop of volume about 5.0 is ejected with a speed of about 3.3 (greater than 0.3 U_n). Larger drops may be ejected with a smaller flow rate. For example, a drop of volume about 9.5 can be generated with $Q = 20$ and $\Delta\tau = 0.5$ at Re = 0.5 with drop shape evolution similar to that in Fig. 12, except that the drop detaches from the nozzle at about $t = 9.0$

and moves at a speed about 1.0. It seems that drops ejected at lower Reynolds number tend to retain their spherical shape better, a likely consequence of the stronger viscous effect that hinders undesirable drop oscillations. With $Q = 20$ and $\Delta\tau = 0.5$ but Re being reduced to 0.3, fluid interface disruption would not occur. At Re = 0.35, an unsuccessful case for drop ejection with $V = 10$ is computed with $Q = 20$ and $\Delta\tau = 0.5$, and shown in Fig. 13, where the drop after slowly detaching from the nozzle moves back and coalesces into the nozzle meniscus. As mentioned before, a higher flow rate Q is needed to generate drops at smaller Reynolds numbers. At Re = 0.1, drop ejection cannot be successful even with $Q = 40$ and $\Delta\tau = 0.25$. An exemplifying case of $Q = 40$ and $\Delta\tau = 0.25$ at Re = 0.125 is shown in Fig. 14 where the drop ejection is successful. Although the average velocity of fluid through the nozzle reaches 12.8 during actuation, the drop speed is very low, about 0.6 in this case. Because the drop size is controlled by $V = Q \Delta\tau$, a higher flow rate and narrower actuation pulse are required for drop ejection as the value of Re decreases.

Concluding Remarks

A variety of drop ejection cases simulated with FLOW-3D in the present work can provide considerable fundamental insights into the factors that control the performance of a drop-on-demand device. By appropriately nondimensionalizing the Navier–Stokes equations that govern the fluid dynamic process of drop ejection,

three dimensionless parameters are identified as control parameters, namely, the Reynolds number (Re), the flow rate during actuation (Q), and duration of the (square) actuation pulse ($\Delta\tau$).

Because of the complexity of the drop ejection process, many detailed features are difficult to define in an exact quantitative sense. Therefore, the analysis here is carried out with numerical accuracies limited to satisfying the immediate practical concerns. The sizes of grid cells used in the VOF computations are designed to be adequately fine for resolving features with length scales greater than $0.1\,L$, i.e., 1 µm for the case of a 20 µm diameter nozzle, but probably not sufficient for quantitative evaluations of the small satellite droplets. The decision of using an $8\,L \times 8\,L$ chamber in the model (cf. Fig. 1) comes from a compromise between the FLOW-3D computational efficiency and the relative insensitivity of the major results to chamber size variations.

To enable drop ejection, the fluid momentum through the nozzle, proportional to $Q^2\,\Delta\tau$, must exceed a critical value that seems to depend on Re and drop volume. For example, at Re = 12.5, the critical value of $Q^2\,\Delta\tau$ appears to be about 50 for $V = 5$ or less, e.g., $Q = 10$ and $\Delta\tau = 0.5$, or $Q = 20$ and $\Delta\tau = 0.125$, etc. As a general trend, the critical value of $Q^2\,\Delta\tau$ for successful drop ejection increases with increasing drop volume or with decreasing Re.

Numerous computed cases indicate that the volume of a successfully ejected drop is fairly close to the volume of fluid pushed through the nozzle during actuation, e.g., within 10% variations, even though the exact position of fluid interface disruption may vary somewhat from case to case. Thus, in designing a drop ejection device, when a desired drop volume is decided, we need to ensure that the device is capable of generating the quantity $V = Q\Delta\tau$ that closely matches the drop volume. Moreover, a certain speed of an ejected drop is also required for ink jet applications. It usually seems desirable to have ejected drops with speeds greater than 5 m/s to achieve good directionality given the variability of wetting forces at the nozzle exit edges.[4] The computational results presented here show that the speed of the ejected drop is typically in a range from one third to two thirds of the average fluid velocity through the nozzle during actuation ($U_n = Q/\pi$). For a given drop volume ($V = Q\Delta\tau$), higher drop speed is obtained with higher flow rate Q and narrower pulse (smaller $\Delta\tau$) of the actuation.

When considering the quality of the ejected drop, large values of Re seem to be undesirable because drops ejected at Re > 5 often disintegrate; many computed results for Re = 5 are very similar to that for Re = 12.5 shown in the Figs. 3–8. It appears to be much easier to generate a round, integrated drop at Re = 1 than at Re = 12.5, as seen in the figures analyzed in this article. According to Eq. 7, reducing Re is equivalent to reducing the size of nozzle (L), or the surface tension (γ), or the density of ink (ρ), or increasing the viscosity of ink (μ). If the reference fluid properties are assumed to be $\gamma = 2.56 \times 10^{-2}$ N/m, $\rho = 10^3$ kg/m^3, and $\mu = 1.6 \times 10^{-2}$ N s/m^2, i.e., that of some non-aqueous inks, we would have Re = 1 (with $L = 10^{-5}$ m, $T = 6.25 \times 10^{-6}$ s, etc.) instead of Re = 12.5 for a typical aqueous ink. However, to eject drops at lower Reynolds number usually requires a higher flow rate, corresponding to more powerful actuation pulse. With the same flow rate Q (for the same V), a drop ejected at smaller Re tends to move at a slower speed. Thus, to obtain a desired drop with desired speed, more powerful actuation is required for cases with smaller Re. If other design constraints make reducing Re impossible, drops ejected at higher flow rates tend to disintegrate at their long tails to generate small satellite droplets, and appear to be less likely to break into large pieces. Again, more powerful actuation seems to yield more desirable results. ⚠

References

1. R. N. Mills, Ink Jet Printing–Past, Present, and Future, in *Proc. IS&T's 10th Int'l. Congress on Adv. in Non-Impact Printing Technologies*, IS&T, Springfield, VA, 1994, pp. 410–414.
2. J. Heinzl and C. H. Hertz, Ink-jet Printing, *Advances in Electronics and Electron Physics*, **65**, 91–171, (1985).
3. E. L. Kyser, L. F. Collins and N. Herbert, Design of an Impulse Ink Jet, *J. Appl. Photographic Eng.* **7** (3), 73–79, (1981).
4. S. F. Pond, Drop-on-Demand Ink Jet Transducer Effectiveness, in *Proc. IS&T's 10th Int'l. Congress on Adv. in Non-Impact Printing Technologies*, IS&T, Springfield, VA, 1994, pp. 414–418.
5. R. R. Allen, J. D. Meyer and W. R. Knight, Thermodynamics and Hydrodynamics of Thermal Ink Jets, *Hewlett-Packard J.* **36**, 21–27 (1985).
6. M. P. O'Horo, N. V. Deshpande and D. J. Drake, Drop Generation Processes in TIJ Printheads, in *Proc. IS&T's 10th Int'l. Congress on Adv. in Non-Impact Printing Technologies*, IS&T, Springfield, VA, 1994, pp. 418–421.
7. S. Kamisuki, T. Hagata, C. Tezuka, Y. Nose, M. Fujii, and M. Atobe, A Low Power, Small, Electrostatically-Driven Commercial Ink Jet Head, in *Proc. IEEE MEMS'98*, IEEE, Heidelberg, Germany 1998, pp. 63–68.
8. F. Pan, J. Kubby and J. Chen, Numerical Simulation of Fluid-Structure Interaction in a MEMS Diaphragm Drop Ejector, *J. Micromech. Microeng.* **12**, 70–76 (2002).
9. G. K. Batchelor, *An Introduction to Fluid Dynamics*, Cambridge University Press, Cambridge, UK, 147–150, 1967.
10. *FLOW-3D User's Manual*, Flow Science, Inc., 1999; www.flow3d.com.
11. C. W. Hirt and B. D. Nichols, Volume of Fluid (VOF) Method for the Dynamics of Free Boundaries, *J. Comput. Phys.* **39**, 201–225 (1981).